Desalination and Water Treatment
www.deswater.com

doi: 10.5004/dwt.2022.28880

273 (2022) 292–307
October

Removal of metoprolol by adsorption onto activated carbon prepared from a food by-product

Djanet Belkharchouche, Naima Gherbi, Abdeslam-Hassen Meniai*

Laboratoire De L'Ingénierie Des Procédés D'Environnement, Université de Constantine 3, Algeria, emails: meniai@yahoo.fr (A.-H. Meniai), beldjanet@yahoo.fr (D. Belkharchouche), naima.gherbi@univ-constantine3.dz (N. Gherbi)

Received 12 March 2022; Accepted 20 August 2022

ABSTRACT

Two activated carbons were prepared by chemical impregnation of bean peels using phosphoric and sulphuric acids, respectively, and tested for the removal of metoprolol from water. Retention capacities of 107.5 and 90 mg/g were achieved for phosphoric and sulphuric acids activated carbons, respectively. These values were by far much higher than 2.98 mg/g, the retention capacity corresponding to raw been peels. The phosphoric acid activated carbon showed the best retention of metoprolol and therefore it was considered to investigate the effects of operating parameters like the adsorbent dosage, the initial concentration, the solution pH, the ionic strength and the temperature. The adsorbent was characterized by pH_{pzc}, thermogravimetric analyses, infrared spectrum and Brunauer–Emmett–Teller analysis. The results of batch metoprolol adsorption onto phosphoric acid activated carbon showed that the optimal solid–liquid ratio was 2 g/L for which the maximum adsorption capacity was 107.5 mg of metoprolol/g of activated carbon, corresponding to a percentage retention efficiency of 98%. The kinetic data showed relatively fast metoprolol sorption onto the phosphoric acid activated carbon, reaching equilibrium in 5 min with initial concentrations lower than 150 mg/L. The results indicated that the adsorption kinetics was well described by the pseudo-second-order model. The adsorption data were best fitted by Langmuir adsorption isotherm model and were also used to calculate thermodynamic parameters like Gibbs free energy, enthalpy and entropy variations.

Keywords: Adsorbent; Bean peels, Metoprolol; Activated carbon; Pharmaceutical pollutant; Adsorption capacity; Activating agents

1. Introduction

It is well established that the pharmaceutical industry is one of the great sources of pollution of the environment, where pharmaceutical compounds are detected with significant concentrations in surface, subsurface and ground waters, domestic and municipal wastewaters, industrial effluents, etc. [1]. These pharmaceutical substances are not biodegradable [2] and cannot be eliminated due to their resistance to conventional wastewater treatments [3]. However, they may be discharged into the aquatic environment and may even reach drinking water intakes [4].

There are several physical and chemical techniques to remove pharmaceuticals compounds from wastewaters. Among these methods, adsorption has shown to be a promising treatment technique, offering advantages such as lower energy consumption and simpler operation conditions in comparison to other tertiary treatments [5].

The adsorption of pharmaceuticals onto natural materials, that is, soils [6], clays [7,8], hydrous oxides [9] and silica [10] has been discussed in details in the literature. Therefore in order to identify potential solid materials as efficient, abundant and low cost adsorbents, the present study focussed on the preparation of an activated carbon (AC)

* Corresponding author.

by chemical impregnation of bean peels (BP), using phosphoric (P) and sulphuric (S) acids, leading to bean peels phosphoric acid and sulphuric acid activated carbons, denoted BPPAC and BPSAC, respectively. The two adsorbents were tested to remove a pharmaceutical pollutant, namely metoprolol, from wastewaters. However BPPAC showed to be more efficient to remove metoprolol which is widely consumed. For example in Germany the estimated metoprolol consumption is between 100–250 tons/y [11]. It is used in moderate hypertension, serious conditions of myocardial infarction, for preventing death of cardiovascular tissue, in angina, tachycardia, extra systole, and for secondary prophylaxis after a heart attack. The most common synonyms are Lopressor, Betaloc, etc. [12].

In fact it is reported in the literature that metoprolol is one of the most frequently analysed beta-blockers in biological and environmental samples with a mobility and a frequent presence in surface waters at high concentrations [13,14] where values outside the 10–100 mg/L range makes it very harmful to aquatic organism [11,15].

Metoprolol may end up in the environment trough excretion from patients taking the medication or disposal of expired unused medication in the toilet, sink, landfill, etc. Clearly these factors have mainly guided the choice of metoprolol in the present study, although metoprolol metabolites such as alpha-hydroxy-metoprolol would also be worth considering later.

Therefore the novelty of the present study is the use and test of bean peels as adsorbent to eliminate, for the first time, a pollutant like metoprolol which may have bad consequences on the aquatic systems, if not taken in charge. Activated carbon was prepared from bean peels, testing phosphoric and sulphuric acids as chemical activating agents.

2. Materials and methods

2.1. Materials

- Bean peels were collected locally. In order to remove any impurities, a first washing stage was carried out followed by an exposure to sun drying. The dried material was sieved to obtain particles of small sizes which were again washed to remove any remaining soluble substance and then dried at a temperature of 110°C for a sufficient time till a constant weight. Finally the material was ground, sieved to obtain particles of diameter less than 0.160 mm and kept in the desiccator, waiting for further use.

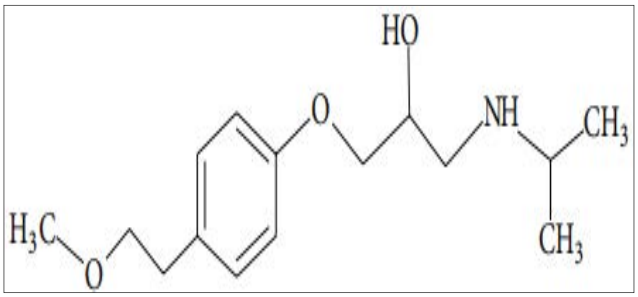

Fig. 1. Metoprolol chemical structure [16].

- Phosphoric acid (85%) was supplied by Cheminova.
- Sulphuric acid (96%) purchased from Carlo Erba Reagents.
- Metoprolol ($C_{15}H_{25}NO_3$) was purchased from Sigma-Aldrich. It is very soluble in water, freely soluble in alcohol, chloroform, and dichloromethane, and slightly soluble in acetone. The molecular structure and further characteristics and are shown in Fig. 1 and Table 1, respectively.

2.2. Methods

2.2.1. Fourier-transform infrared spectroscopy

Fourier-transform infrared spectroscopy (FTIR) analyses were performed to identify the chemical functions of the solid support surface by means of a JASCO FT/IR apparatus. The classical procedure was used and consisted in well mixing solid samples with potassium bromide at a weight ratio of 1:10. The obtention of scans was at a resolution of 4 cm^{-1}, from 4,000 to 400 cm^{-1}.

2.2.2. pH_{pzc}

A JENWAY pH-meter type 3510 apparatus was used in order to determine the pH_{pzc} at the point of zero charge. Any pH higher than the pH_{pzc} corresponded to a negatively charged adsorbent surface. The used pH_{pzc} determination classical procedure was well described by Gherbi et al. [17].

2.2.3. Thermogravimetric analysis

The thermal degradation of the chemically treated bean peels as well as a comparison with raw BP, were examined by means of a thermogravimetric analysis using STA 449 F3 Jupiter thermogravimetric analyser.

2.2.4. Activation procedure

Activated carbons were produced from natural BP which is a cellulose-based material. In a previous study raw BP showed a very high retention efficiency of Rhodamine [17], contrary to the case of metoprolol where the retention was relatively low, hence the need of an activation process. Thus the purpose of the present work was to produce an activated carbon by chemical activation of BP, with suitable reagents, hence avoiding the preliminary stage of raw BP carbonization and leading to the production of activated carbon characterized by a higher performance and an enhanced development of the porous

Table 1
Physico-chemical and proprieties of metoprolol [11]

Physico-chemical propriety	Value
Density (g/cm³)	1.0 ± 0.1
Water solubility at 25°C (mg/L)	16,900
M (g/mol)	267.36
pKa	9.52
Toxicity (mg/kg)	3,090 < LD_{50} < 4,670

structure [18]. A priori, the activation process of BP was carried out by impregnation, testing the two considered chemical agents (phosphoric acid and sulphuric acid). The experimental procedures for activation with H_3PO_4 and H_2SO_4 were described in details in the literature [19–22], and briefly they are as follows:

- Phosphoric acid bean peels activation: dried raw BP was impregnated with a weighted amount of H_3PO_4 in aqueous solution, at an impregnation ratio, defined as the ratio of the weight of H_3PO_4 (g) to that of the precursor, of 200% (on weight basis). After drying at 110°C for 24 h, samples were then heated for 1 h at 450°C at a heating rate of 10°C/min. The residual phosphoric acid was eliminated from the activated carbons by washing with distilled water until no phosphate ions were detected in the water by a lead nitrate test. After drying at 110°C for 24 h, the final material was then grounded and sieved to obtain particles with diameter < 0.16 mm [21];
- Sulphuric acid bean peels activation: similarly to the phosphoric acid activation and still at an impregnation ratio of 200%, dried raw BP was impregnated with sulphuric acid at ambient temperature and the resulting mixture was heated up to 200°C, before being washed to eliminate any residual acid [22].

It should be noted that once the results showed that BPPAC was by far more efficient than BPSAC to retain metoprolol, it was characterized according to the classical procedure, involving thermogravimetric analyses (TGA), infrared spectroscopy, pH measurement of the point of zero charge (pH_{pzc}) and Brunauer–Emmett–Teller (BET).

2.2.5. Adsorption procedure

The adsorption experiments were carried out batchwise at ambient temperature of 20°C ± 2°C by mixing various amounts of the activated carbon in the range of (0.001–0.05 g) in 100 mL of metoprolol solutions with concentrations varying from 10 to 280 mg/L at various pH (2–12). The mixture was continuously agitated at a speed of 200 rpm and the resulting suspension was then centrifuged at 5,000 rpm during 10 min. The final solution of metoprolol was analysed using UV/visible spectrophotometer (UV-1601 Shimadzu) set at a wavelength λ_{max} 222 nm. The changes of absorbance were determined at time intervals from 5 to 250 min, during the adsorption process. The adsorbed metoprolol amount at equilibrium, q_e (mg/g), was calculated using the following equation:

$$q_e\left(\frac{\text{mg}}{\text{g}}\right)=\frac{C_0-C_t}{r} \tag{1}$$

where C_0 and C_t are the concentrations (mg/L) of metoprolol in solution before and after adsorption, respectively and r (g/L) is the solid/liquid ratio of bean peels.

2.2.6. Desorption cycles of generation

Desorption experiments were performed with the different considered solvents. All experiments were carried out after saturation of the activated carbon with an initial concentration of metoprolol of 250 mg/L and at the optimal adsorbent dose of 2 g/L. The suspension was stirred during 120 min then BPPAC was filtered and dried at 110°C for 24 h, ready for the next cycle of desorption.

2.2.7. Brunauer–Emmett–Teller

The prepared activated carbon was characterized by physical adsorption of gases (N_2 at 77.35 K) according to the known protocol, using a Quantachrome Instruments Version 5.21 – Automated Gas Nitrogen adsorption.

3. Results and discussion

3.1. BET results

The N_2 isotherms adsorption shown in Fig. 2 are of type V, typically characteristic of mesoporous solids undergoing capillary condensation and hysteresis during desorption [23], similarly to H_2O isotherm on SBA-15 (mesoporous silica material known as Santa Barbara Amorphous-15) at 290 K [24].

The specific surface areas obtained for BP, BPSAC and BPPAC were 0.422, 38.25 and 1,100.39 m^2/g, respectively. Clearly the activation process had improved the specific surface area of the adsorbent, particularly for BPPAC by a factor of 2,600.

For a comparison purpose, the specific surface area obtained for BPPAC was close to 1,210; 925 and 1,112 m^2/g, values obtained for steam CFS36 activated carbon fibers [25], activated coffee grounds CGAC180 [21] and commercial activated carbon WG-12 obtained from special – low ash – coking coal and a binder [18], respectively.

Due to the great specific area of BPPAC, there was no need to consider further BPSAC in the rest of the study.

3.2. pH_{pcz} measurement

Fig. 3 shows an amphoteric character of BPPAC surface where the charge changes with the pH value. For a pH below and above 4, the surface was positively and negatively charged, respectively.

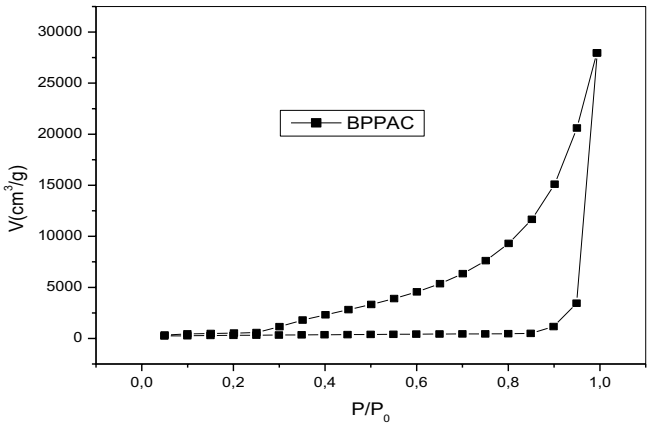

Fig. 2. Adsorption–desorption isotherms of nitrogen at 77 K on BPPAC.

3.3. FTIR spectroscopy analysis

In order to explore the surface characteristics of BPPAC a Fourier-transform infrared (FTIR) analysis was performed in the range of 450–4,000 cm^{-1}. Fig. 4 shows the FTIR spectra of BPPAC. The peaks at major absorption bands were observed at: 1,740 cm^{-1} corresponding to (–C=O) of ketones; aldehydes or carboxylic groups [2]; 1,580 cm^{-1} representing –C=C– vibrations of aromatic cycles [21]; 1,050 cm^{-1} reflecting asymmetric stretch of –C–O–C– [26]; 1,200 cm^{-1} signifying functional group of =C–O–C. The band at 2,350 cm^{-1} characterises –OH of carboxylic groups [21] and 3,750 cm^{-1} of stretch vibration of bonded hydroxyl group in the phenolic groups [27].

3.4. TGA analysis

Fig. 5 represents the thermal degradation of the chemically treated bean peels as well as a comparison with raw BP. Thermal degradation of BPPAC occurred at lower temperatures in comparison to raw bagasse, with just only one similarity of a mass decrease in the first interval of 20°C–120°C due to water evaporation [28]. Beyond 400°C, the second significant mass loss of BPPAC was due to volatilisation of various hydrocarbons matter and carbon oxides, caused by hydrolysis of the lignocellulosic material in BP during H_3PO_4 impregnation [29]. The third weight loss at temperatures between 400°C and 800°C for BPPAC was due to evaporation of polyphosphoric acids (H_3PO_4, $H_4P_2O_7$ and $H_5P_3O_{10}$) which were formed through the condensation of the impregnated phosphoric acid by water loss [28,30].

3.5. Scanning electron microscopy

Scanning electron microscopy (SEM) characterization was obtained at a resolution using a particle size less than 62 μm. The results presented in Fig. 6 indicate that the BPPAC had an heterogeneous porous nature with pore sizes between 5–30 μm. For a comparison purpose, these were much larger than those created in BPSAC as shown in Fig. 7.

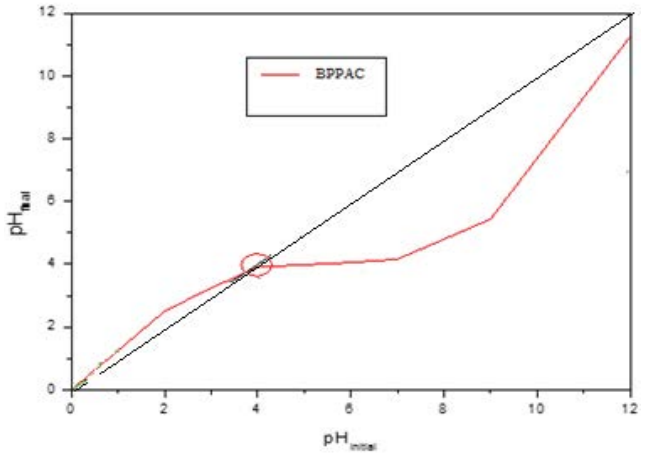

Fig. 3. Plot of pH_{pzc} of BPPAC.

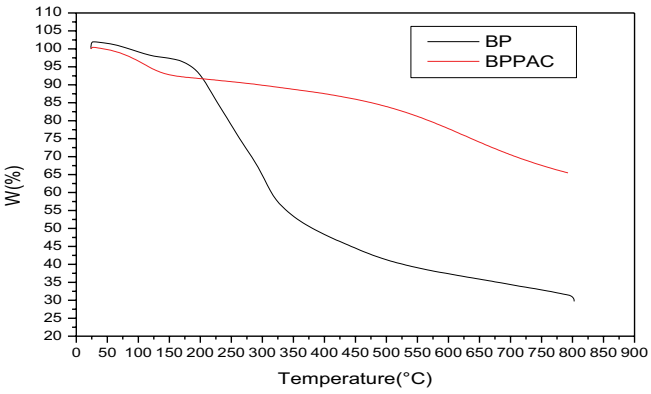

Fig. 5. TGA analysis of BPPAC.

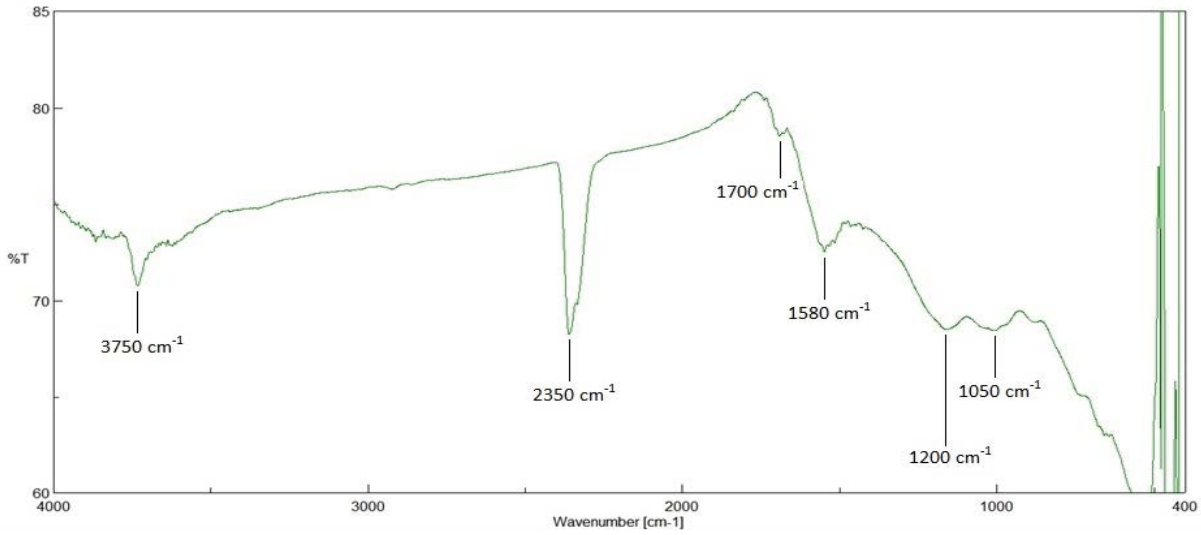

Fig. 4. IR spectra of BPPAC.

3.6. Effect of the activating agent

The effect of this important parameter is shown in Fig. 8 where it can be noticed that the BP adsorption capacity of metoprolol (2.98 mg/g) was very low when compared with phosphoric acid activated carbon (BPPAC). The specific surface area developed by phosphoric acid was larger, due to large pore sizes at the surface as the activation by phosphoric acid promoted the formation of mesopores [21]. This was confirmed by the work reported by Mirzaee et al. [31] who similarly considered the preparation of an activated carbon from an agriculture waste still by means of phosphoric acid as the activating agent and physical activation to remove diclofenac from wastewaters, by adsorption.

Clearly Fig. 8 shows that the retention capacity by BPPAC was greater than that obtained by BP and BPSAC. This was similar to results shown by Jaafarzadeh et al. [32] who produced activated carbon from Milk-vetch (MV) waste with an adsorption capacity of Bisphenol A higher than that of commercial activated carbon.

3.7. Effect of solid/liquid ratio on equilibrium adsorption capacity and removal efficiency

In order to examine the influence of the solid/liquid ratio on the adsorption capacity (q_e) and the percentage of elimination (R%), the adsorbent dose was varied from 0.25 to 10 g/L, while maintaining the initial concentration of metoprolol constant at 200 mg/L, as well as other operating parameters like contacting time, temperature and agitation speed. Fig. 9 shows that the adsorbed amount of metoprolol decreased from 182 to 24 mg/g with the increase of solid/liquid ratio from 0.25 to 10 g/L. This might be due to the decrease in the total sorption surface area available to metoprolol [33] resulting from overlapping or aggregation of sorption sites [34]. The elimination percentage (R%) increased with adsorbent dose from 16% to 98% and this was due to surface sites of the adsorbent increase upon increasing the adsorbent dosage. For an adsorbent dose above 2 g/L of, there was no significant increase in the removal rate. Regarding q_e and R%, an adsorbent dose of 2 g/L showed

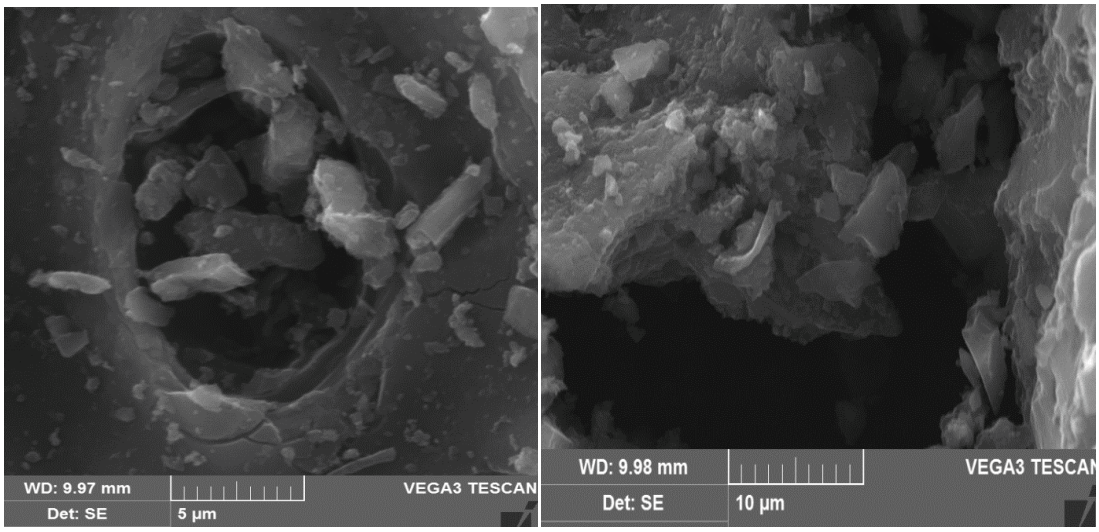

Fig. 6. SEM images of BPPAC.

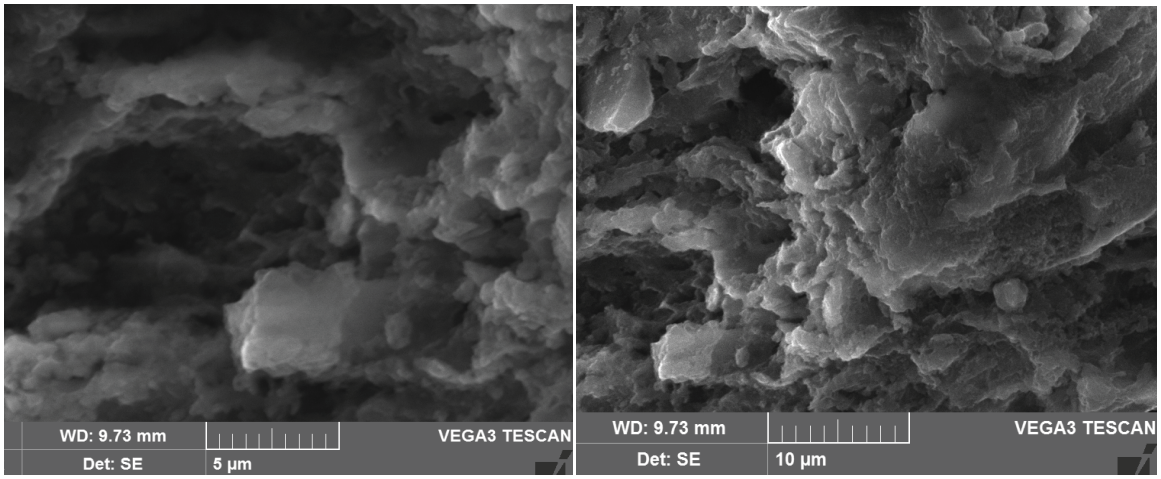

Fig. 7. SEM images of BPSAC.

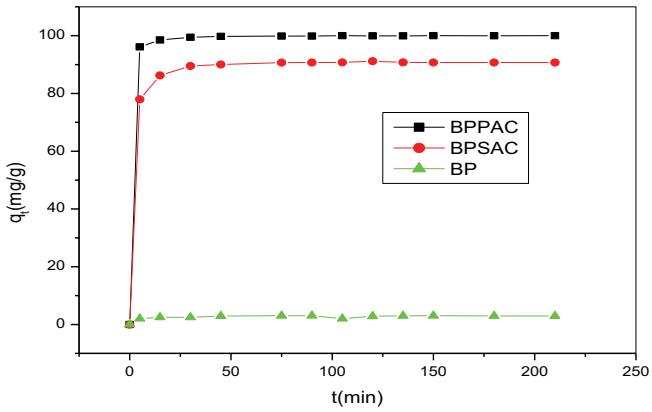

Fig. 8. Effect of the activating agent of BP on retention of metoprolol.

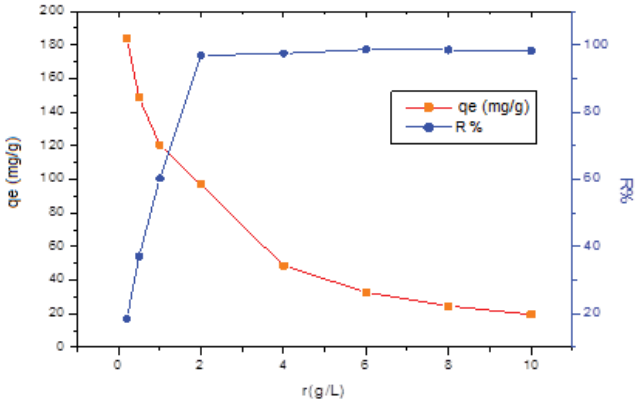

Fig. 9. Effect of adsorbent dose of BPPAC on equilibrium adsorption capacity and removal efficiency of metoprolol.

to be the optimum value and was used for all further experiments.

3.8. Effect of initial concentration on kinetics and adsorbed quantity

To study the effect of the initial concentration of metoprolol on adsorption capacity by BPPAC, experiments were carried out by varying the adsorbate concentration in the range from 20 to 200 mg/L. The results shown in Fig. 10 indicate that the increase in the initial concentration from 20 to 200 mg/L led to an increase in adsorption capacity from 8.97 to 100 mg/g, respectively. This can be explained by the fact that when the initial concentrations increased, the mass transfer driving force became larger and the interactions between metoprolol and BPPAC were enhanced [35], hence resulting in higher adsorption capacity. This result was commonly observed in adsorption of medical molecules such as ketoprofen [36] or dye molecules for Crystal violet (CV) [37,38]. It can also be observed that the initial metoprolol concentration affected the equilibrium time. The retentions were instantaneous for concentrations lower than 100 mg/L; for 150 mg/L and for 200 mg/L equilibrium was reached after 15 min. This was probably due to the

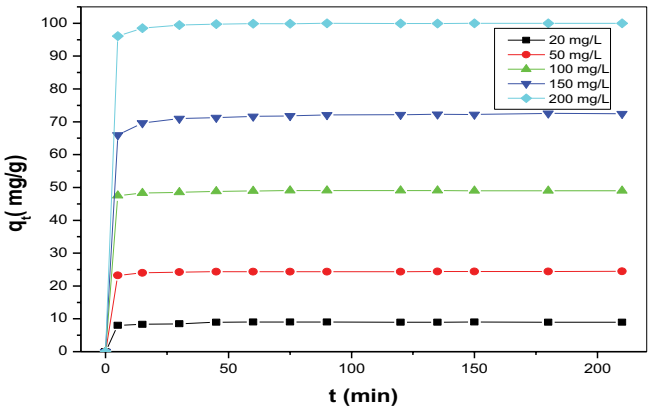

Fig. 10. Effect of initial concentration on kinetics and adsorbed quantity of metoprolol.

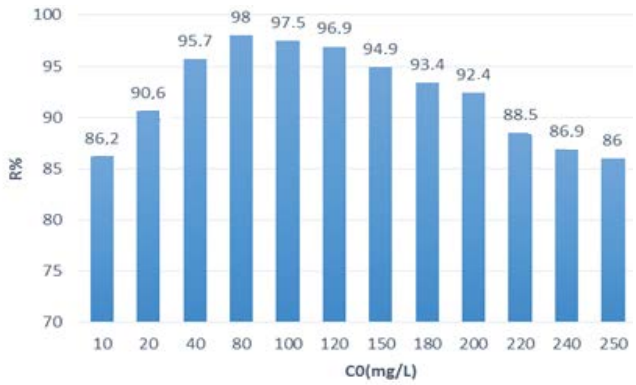

Fig. 11. Effect of initial concentration on removal efficiency at equilibrium time.

saturation of the adsorption sites, as well as to the repulsive forces between the adsorbed and free molecules [39].

From Fig. 11 it is noted that the BPPAC was effective through all the interval of the initial concentrations ranging from 10 to 250 mg/L. The removal efficiency was greater than 86% and reached its maximum value of 98% for an initial concentration of 80 mg/L, in agreement with the result reported by Singh et al. [22].

3.9. Effect of initial pH

To study the effect of initial pH of the solution on the adsorption of metoprolol onto BPPAC, the experiments were carried out at different pH values varying from 2 to 12. The results of Fig. 12 indicate that in an acidic medium ($2 < pH \leq 4$) the adsorbed amount of metoprolol was not affected by pH and remained constant in this interval at 78.38 mg/g. In the pH range between 4 and 10 an increase in the adsorbed amount of metoprolol was noted from 78.38 to a maximum of 94.548 mg/g at pH 10. This may be explained by the electrostatic attraction forces induced between negative surface charges of BPPAC ($pH > pH_{pzc} = 4$) and positively charged groups of metoprolol ($pH < pK_a = 9.5$). With increasing pH ($pH > pKa = 9.5$) the removal of metoprolol decreased, probably due to repulsive forces between

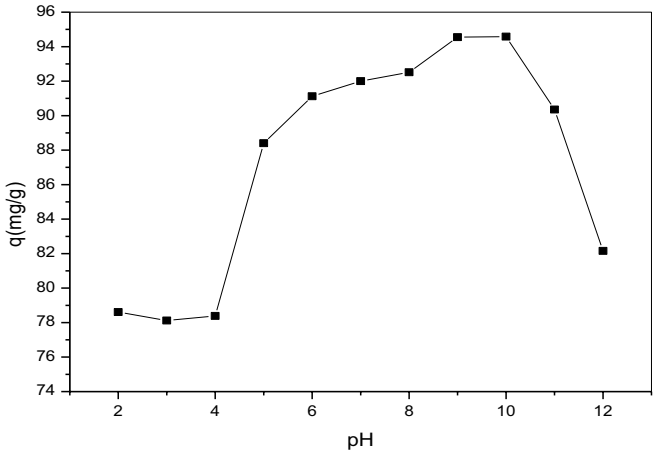

Fig. 12. Effect of initial pH of solution on the adsorption of metoprolol.

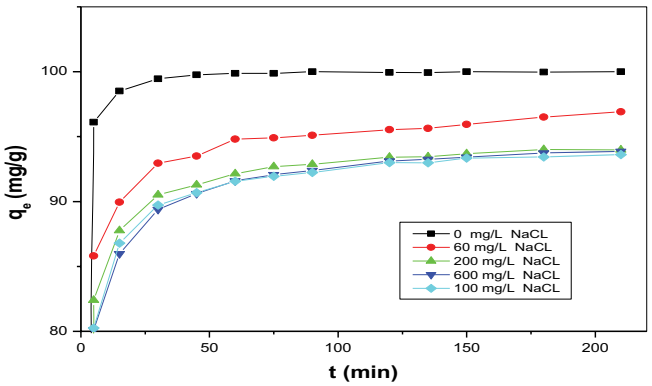

Fig. 13. Effect of sodium chloride (NaCl) on the adsorption of metoprolol.

negative surface charge of BPPAC (pH > pH_{pzc} = 4) and negatively charged groups of metoprolol, confirming the result obtained by Naghipour et al. [40].

3.10. Effect of sodium chloride

The influence of salt ionic strength on the adsorption capacity is important, since large amounts of salts are commonly present in wastewater [41]. Effect of salinity on adsorption of metoprolol was tested by using NaCl at different concentrations ranging from 60 to 1,000 mg/L. The results of Fig. 13 show that the adsorbed amount of metoprolol decreased in presence of NaCl because an increase in ionic strength leads to a decrease in electrical double layer (EDL) thickness and an increase in the amount of indifferent ions approaching the BPPAC surface. Thus, the results shown above can partly be attributed to an increased competition between metoprolol and Na^+ ions for surface sites with increasing the ionic strength [42]. Similar results were reported using different adsorbents for the removal of dyes and medical wastes [43].

3.11. Comparison of metoprolol retention onto different adsorbents

In order to assess the performance of BPPAC to eliminate metoprolol, a comparison with results reported in the literature concerning the same task but by means of different adsorbents, is shown in Table 2.

It is very clear that the removal rate percentage (98%) achieved by BPPAC in the shortest time, was among the highest and equal to that shown by another adsorbent (*Spirulina*-based activated carbon [45]), hence confirming the efficiency of the activated process adopted in the present work, particularly the judicious choice of phosphoric acid as the activated agent.

3.12. Kinetics study

Adsorption kinetics should be investigated in order to illustrate how the solute uptake rate control the residence time of the adsorbate at the solution interface and also to elucidate the mechanism of the adsorption process, which is dependent on the physical and chemical characteristics of the adsorbent and experimental system.

The capability of pseudo-first-order, pseudo-second-order, modified Freundlich, Elovich, intraparticle diffusional and film-diffusion models to represent the kinetics data, was examined in this study for five different initial concentrations of metoprolol (20, 50,100 ,150 and 200 mg/L) at constant temperature of 20°C.

- The linear form of pseudo-first-order model of Lagergren is generally expressed as follows [23]:

$$\ln\left(q_e - q_t\right) = \ln q_e - K_1 t \tag{2}$$

where K_1 (min^{-1}) is the pseudo-first-order adsorption kinetics rate constant, q_t the adsorption capacity at time t and q_e the adsorption capacity at equilibrium. Slope and intercept of $\ln(q_e - q_t)$ vs. t give the values of K_1 and q_e, respectively.

- The pseudo-second-order model is given as follows [46,47]:

$$\frac{t}{q_t} = \frac{1}{K_2 q_e^2} + \frac{1}{q_e^2} t \tag{3}$$

where K_2 is the second-order adsorption kinetics rate constant. Values of K_2 and equilibrium adsorption capacity (q_e) were obtained from the intercept and slope of the plots of t/q_t vs. t, respectively according to Eqn. (3).

- Weber and Morris proposed a model to explain the intraparticle diffusion during the adsorption process [48] which is related to the transport of metoprolol from its aqueous media to the pores of the adsorbent. This is expressed as:

$$q_t = K_{int} t^{1/2} + C \tag{4}$$

where K_{int} the intraparticle diffusion constant and C is a constant related to layer thickness [48,49].

Table 2
Comparison of BPPAC and other activated carbon efficiencies

Adsorbent	Removal rate %	Operating conditions	Reference
Bean peel phosphoric acid activated carbon	98	T = 20°C; pH = 9.5; r = 2 g/L; $C0$ = 150 mg/L, t = 5 min, d = 0.16 mm	This work
Sepiolite-supported nanoscale zero-valent iron (SPT-nZVI)	67.24 ± 0.95	$C0$ = 3 mg/L (10 mM H2O2), r = 0.5 g/L, pH = 3, t = 60 min. Case I: Absence of water anions and cations	[44]
	55.16 ± 1.26	Case II: Presence of water anions and cations	
Activated carbon prepared from pine cones	89.2	T = 25°C, pH = 8.5, r = 1.5 g/L, t = 60 min, and $C0$ = 50 mg/L	[40]
Activated *Spirulina*-based carbon material	98	T = 25°C, pH = 5.9, r = 0.25 g/L, $C0$ = 1 mg/L, t = 20 min	[45]

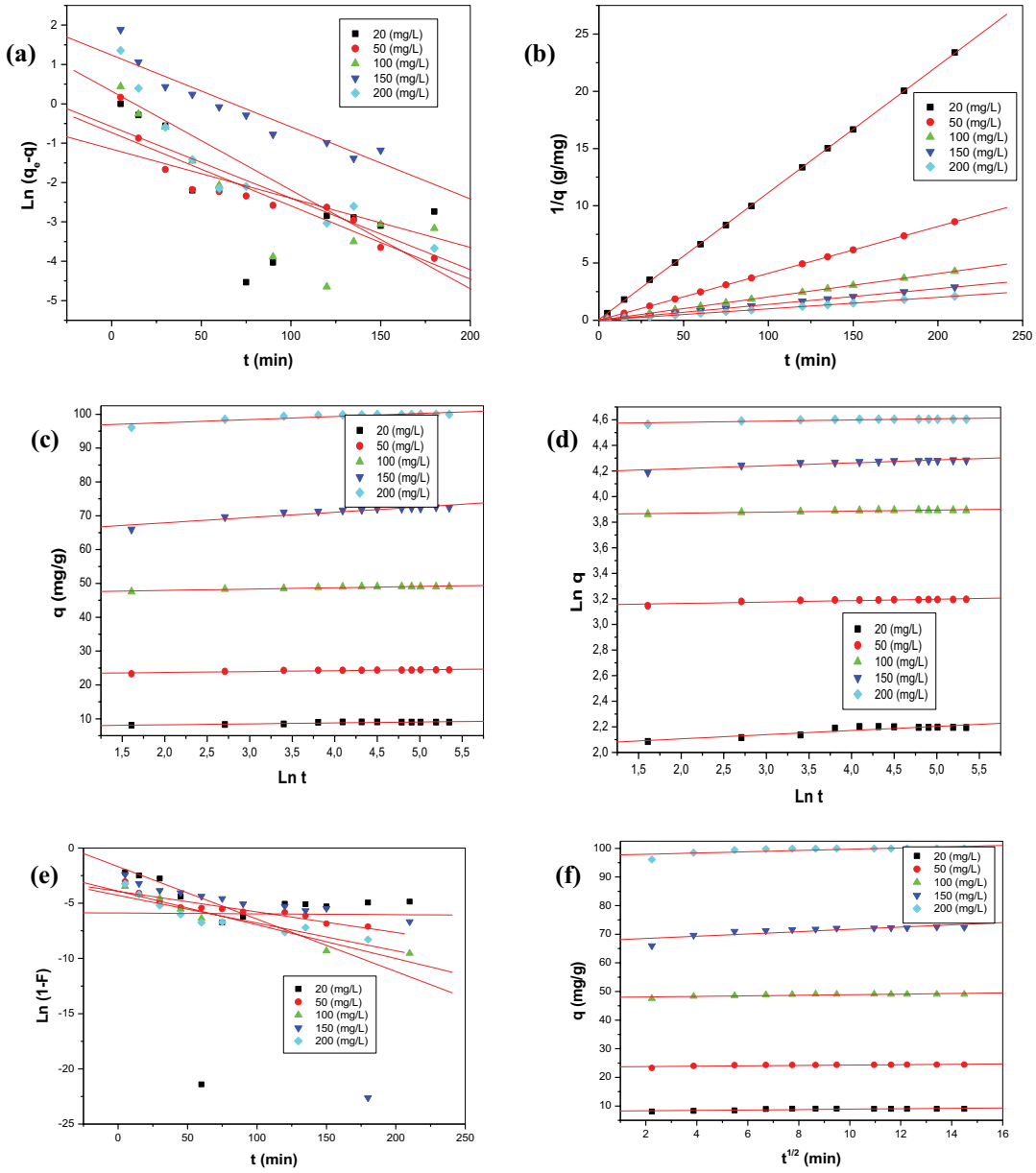

Fig. 14. Kinetics data plots for metoprolol retention on BPPAC: (a) pseudo-first-order model equation, (b) pseudo-second-order model, (c) Elovich, (d) modified Freundlich, (e) film-diffusion, and (f) intraparticle diffusion models.

- Modified Freundlich model: the linear form of this model is given as [50]:

$$\ln q_t = \ln\left(k_f C_0\right) + \frac{1}{m}\ln t \quad (5)$$

where C_0 is the initial concentration (mg/L) of metoprolol, k_f is the apparent adsorption rate constant (L/g·min), and m is the Kuo–Lotse constant. The values of k_f and m were used to evaluate the influence of the ionic strength on the adsorption process. The values of m and k_f were measured from the slope and the intercept of $\ln q_t$ vs. t plot [51].

- Elovich model [52] is generally expressed as:

$$q_t = \left(\frac{1}{\beta}\right)\ln\left(\alpha\beta\right) + \left(\frac{1}{\beta}\right)\ln t \quad (6)$$

where α is the initial adsorption rate (mg/g·min) and β is the desorption constant (g/mg). A plot of q_t vs. ln$t$ leads to a linear relationship with slope (1/β) and intercept 1/β ln(α·β).

- The film-diffusion model is expressed as:

$$\ln\left(1-F\right) = -k_{fd}t \quad (7)$$

where $F = (q_t/q_e)$ and k_{fd} is the liquid film-diffusion constant. The adsorption process follows the film-diffusion mechanism when the plots of $-\ln(1 - q_t/q_e)$ vs. t at different initial concentrations are linear or nonlinear but do not pass through the origin [53].

Mass transfer from the bulk liquid to the solid surface is assumed the slowest step. Moreover, mechanical mixing with the rapid and constant stirring of the solution eliminates the effect of transport [54].

By comparing the data presented in Table 3, the R^2 values for the pseudo-second-order model were higher than those of the other models, suggesting that this model is the best to represent kinetic data.

3.13. Isotherm analysis and modeling

Equilibrium adsorption isotherm is of fundamental importance in the design of adsorption systems. In order to define the type of isotherm, the amount of metoprolol adsorbed at equilibrium as a function of the concentration of the equilibrium solution for initial concentration interval (10–300 mg/L), was plotted. All adsorption experiments were carried out at three different temperatures (20°C, 30°C and 50°C) using a batch technique at a fixed pH.

According to Charles and Hill classification, the curve shown in Fig. 15 forms 'L shape' class (L2) [55], indicating

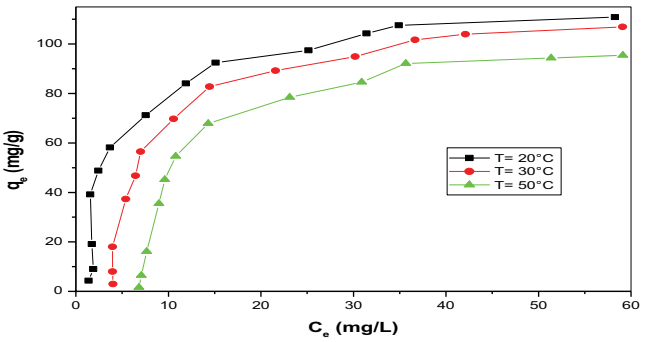

Fig. 15. Adsorption isotherm of metoprolol onto BPPAC at different temperature.

Table 3
Parameters of the kinetic models for metoprolol adsorption

C_0 (mg/L)		20	50	100	150	200
$q_{e,exp}$ (mg/g)		9.045589	24.4383	49.0624	72.5519	100
Pseudo-first-order model	K_1	0.02878	7.2084×10^{-3}	0.0110	0.04548	0.023836
	R^2	0.33708	0.39801	0.467978	0.50249	0.36914
	$q_{e,cal}$	0.316984	2.525×10^{10}	9.7493×10^{20}	1.4222×10^{30}	5.9548×10^{42}
Pseudo-second-order model	K_2	1.47962	3.30024	5.33246	1.29962	5.67613
	R^2	0.99991	1	1	1	1
	$q_{e,cal}$	9.02882	24.45579	49.09104	72.72712	100.10002
Modified Freundlich	k_f	0.38506	0.46314	0.47161	0.43274	0.47866
	R^2	0.8207	0.79197	0.87268	0.87627	0.78671
	M	30.7881	90.4977	123.1527	44.4839	108.6956
Elovich	B	3.5944	3.7870	2.5449	0.63922	1.10593
	R^2	0.81711	0.79605	0.87402	0.8842	0.78941
	A	2.558×10^{11}	3.122×10^{37}	5.0736×10^{51}	1.5128×10^{18}	8.4315×10^{45}
Film-diffusion	k_{fd}	0.04389	0.05151	0.05792	0.05986	0.05986
	R^2	$9.95.10^{-5}$	0.85503	0.93904	0.35073	0.35073
Intraparticle diffusion	K_{int}	0.07114	0.06475	0.09905	0.39766	0.21883
	C	8.18196	23.6658	47.89373	67.7215	97.50498
	R^2	0.63788	0.57142	0.66315	0.68211	0.55205

that metoprolol molecules were probably adsorbed in flat position due to low competition between the adsorbate and solvent molecules [56,57]. It can also be observed that the equilibrium adsorption capacity decreased with increasing temperature (Fig. 15) from 20°C to 50°C. This was mainly due to the decreased surface activity indicating that the adsorption of metoprolol by BPPAC was exothermic in nature [58]. The same behaviour was observed for L-phenylalanine retention by ACK and ACZ [59], and for Rhodamine B adsorption onto WO3/AC [60].

To describe the equilibrium adsorption systems, sorption data obtained with variations of metoprolol concentrations were treated using Langmuir, Freundlich, Temkin, Dubinin–Radushkevich, Elovich and BET isotherm models. These are expressed by the equations listed in Table 3 along with their linear forms and the fitted parameters shown in Tables 4 and 5, respectively.

- The Langmuir model [61] assumes uniform energies of adsorption onto the surface and no transmigration of adsorbate in the plane of the surface, where q_e is the amount adsorbed at equilibrium (mg/g) and C_e is the equilibrium concentration of solute in solution (mg/L) and b is a constant related to the energy of adsorption (L/mg). The equation can be linearized to five different linear forms as shown in Table 4.

In fact it should be noted that for the Langmuir models, the use of the non-linear rather than the linear forms may be preferable since the fitting errors are generally minimized. However the advantage of the latters is the fact that they enable the calculation of the model constants easily.

- The Freundlich expression is an exponential equation and therefore, indicates that as the adsorbate concentration increases, the concentration of adsorbate on the adsorbent surface also increases. Freundlich treatment gives the parameters n indicative of bond energies between metal ions and the adsorbent and k_f (mg/g) related to bond strength [62].
- Temkin equation which is a correction of Langmuir equation by introducing the influence of temperature on the adsorption [63], assumes that the adsorption energy of all molecules involves a uniform distribution of the maximum binding energy, and further indicates that the decrease in adsorption heat is linear rather than logarithmic [64], where b_T is the Temkin constant, K_T (L/g) is the equilibrium bond constant, R (kJ·mol/L·K) is the universal gas constant and T (K) is the temperature.
- Dubinin–Radushkevich isotherm is generally applied to describe the adsorption mechanism onto a heterogeneous surface by a Gaussian energy distribution [65] where X'_m (mg/g) is the theoretical isotherm saturation

Table 4
Isotherm models equation and their linear forms

Langmuir	Type 1		$\frac{1}{q_e}=\frac{1}{q_m}+\frac{1}{bq_m}\frac{1}{C_e}$	$\frac{1}{q_e}=f\left(\frac{1}{C_e}\right)$
	Type 2		$\frac{C_e}{q_e}=\frac{1}{bq_m}+\frac{1}{q_m}C_e$	$\frac{C_e}{q_e}=f\left(C_e\right)$
	Type 3	$q_e=\frac{q_m bc_e}{1+bc_e}$	$q_e=-\frac{q_e}{C_e}\frac{1}{b}+q_m$	$q_e=f\left(\frac{q_e}{C_e}\right)$
	Type 4		$\frac{q_e}{C_e}=-bq_e+bq_m$	$\frac{q_e}{C_e}=f\left(q_e\right)$
	Type 5		$\frac{1}{C_e}=bq_m\frac{1}{q_e}-b$	$\frac{1}{C_e}=f\left(\frac{1}{q_e}\right)$
Freundlich		$q=k_f c_e^{1/n}$	$\log q_e=\log K+\frac{1}{n}\log C_e$	$\log q_e=f\left(\log C_e\right)$
Temkin		$q_e=\frac{RT}{b_T}\ln\left(K_T C_e\right)$	$q_e=B\ln Kt+B\ln C_e$	$q_e=f\left(\ln C_e\right)$
Dubinin–Radushkevich		$q_e=X'_m\exp\left(-K'\varepsilon^2\right)$	$\ln q_e=\ln X'_m-K'\varepsilon^2$	$\ln q_e=f\left(X'_m\right)$
Elovich		$\frac{q_e}{q_m}=K_e C_e\exp\left(\frac{-q_e}{q_m}\right)$	$\ln\frac{q_e}{C_e}=\ln K_e q_m-\frac{q_e}{q_m}$	$\ln\frac{q_e}{C_e}=f\left(q_e\right)$
BET		$\frac{q}{q_m}=\frac{K\left(\frac{C}{C_0}\right)}{\left(1-\frac{C}{C_0}\right)\left[1+\left(K-1\right)\frac{C}{C_0}\right]}$	$\frac{C_e}{q_e\left(C_0-C_e\right)}=\frac{1}{q_m K}+\frac{K-1}{q_m K}\left[\frac{C_e}{C_0}\right]$	$\frac{C_e}{q\left(C_0-C_e\right)}=f\left(\frac{C_e}{C_0}\right)$

Table 5
Parameters of Langmuir, Freundlich and Dubinin–Radushkevich isotherms

Models	Parameters	T = 20°C	T = 30°C	T = 50°C
		q_{ex} = 110.867	q_{ex} = 106.926	q_{ex} = 95.444
	q_m	107.181	153.139	157.480
Langmuir 1	b	0.355	0.0673	0.0390
	R^2	0.993	0.9413	0.904
	q_m	113.122	133.511	114.285
Langmuir 2	b	0.2932	0.0887	0.0932
	R^2	0.998	0.982	0.995
	q_m	323.091	1,438.1	1,778.02
Langmuir 3	b	0.338	0.0917	0.0692
	R^2	0.9799	0.8065	0.9149
	q_m	109.96	146.07	127.34
Langmuir 4	b	0.3312	0.0739	0.0633
	R^2	0.9799	0.8065	0.9149
	q_m	107.627	160.70	120.26
Langmuir 5	b	0.352	0.0593	0.0776
	R^2	0.993	0.971	0.990
	k_f	36.4197	19.7016	20.4339
Freundlich	n	3.1277	2.0942	2.5012
	R^2	0.9792	0.9127	0.9241
	K' (mol²/J²)	–3.9099	–34.0439	–74.2008
Dubinin–Radushkevich	q_m (mg/g)	89.9667	98.8595	94.8218
	R^2	0.8689	0.9908	0 .9848

capacity, K' (mol²/kJ²) is the Dubinin–Radushkevich constant, ε is the Polanyi potential, R is the gas constant and T (K) is the absolute temperature.

- Elovich model is supported by a kinetic principle assuming that the adsorption sites increase exponentially with adsorption, which implies a multilayer adsorption [66]. K_E is the Elovich equilibrium constant (L/mg) and q_m is the Elovich maximum adsorption capacity (mg/g).
- BET models assumed that a number of layers of adsorbate molecules form at the surface of adsorbent and that the Langmuir equation is applied to each layer of adsorption, with q_m is the maximum adsorption capacity (mg/g) and K is BET constant and C_0 the initial concentration (mg/L).

Clearly from Fig. 15 the process shows a saturation plateau behavior in favor of Langmuir models rather than a multilayer adsorption process which is well described by models like BET. Therefore there was not need to consider this model further. Temkin and Elovich models showed relatively determination coefficients, therefore they were also discarded. The values of the different constants of each retained model are shown in Table 5 and the isotherm plots are presented in Fig. 16a–f.

By analyzing these results, it can be observed that the second linear Langmuir equation exhibited the best fit of experimental equilibrium data with high determination coefficients (R^2 = 0.982–0.995) for the three temperatures, suggesting a monolayer adsorption of metoprolol [39]. The n values of Freundlich isotherm were higher than unity, implying that the adsorption of metoprolol on BPPAC was a favorable physical process for all temperatures [67].

3.14. Adsorption thermodynamic studies

To ascertain whether the adsorption process was endothermic or exothermic, thermodynamic data such as free energy change ΔG° (kJ/mol), enthalpy change ΔH° (kJ/mol) and entropy change ΔS° (kJ/mol·K), were evaluated with respect to the feasibility and spontaneous nature of the adsorption process. They can be estimated by equilibrium constants changing with temperature as shown by Eqs. (8)–(11) [68,69]:

$$K_{ad} = \frac{C_{Ae}}{C_e} \tag{8}$$

$$\Delta G^\circ = -RT \ln K_{ad} \tag{9}$$

$$\Delta G^\circ = \Delta H^\circ - T\Delta S^\circ \tag{10}$$

$$\log K_{ad} = \frac{\Delta S^\circ}{2.303R} - \frac{\Delta H^\circ}{2.303RT} \tag{11}$$

where K_{ad} is the equilibrium constant, C_e is the equilibrium concentration in solution (mg/L) and C_{Ae} is the amount of metoprolol adsorbed from the solution at

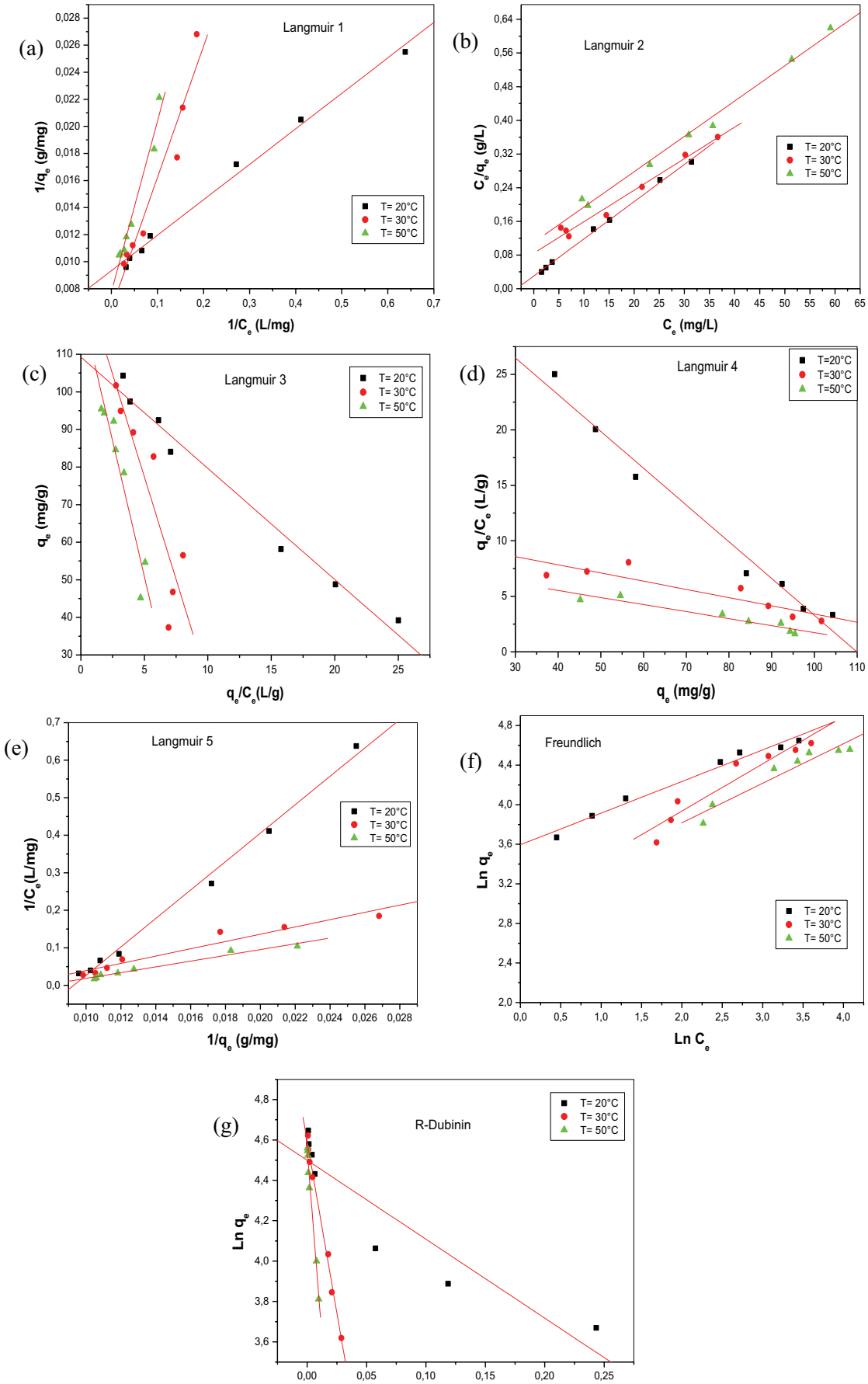

Fig. 16. Isotherm of metoprolol adsorption onto BPPAC (T = 20°C, 30°C, and 50°C): (a) Langmuir 1, (b) Langmuir 2, (c) Langmuir 3, (d) Langmuir 4, (e) Langmuir 5, (f) Freundlich, and (g) Dubinin–Radushkevich.

equilibrium (mg/L), R is the universal gas constant (8.314 J/mol·K), T is the absolute temperature (K). However the approach proposed in this work may also be regarded as valid and is confirmed by studies reported in the literature Fujiwara et al. [68].

The advantage of this approach is to preserve the fact that K_{ad} is expressing a sort of solute partition between the liquid solution and the solid adsorbent, since for a given solid to liquid ratio (r) C_{Ae} is equal to (C_0 (mg/L) – C_e (mg/L)), with C_0 (mg/L) and C_e (mg/L), the initial and the equilibrium concentrations, respectively, and may be regarded as an equivalent way to express the concentration of adsorbate in adsorbent via Eq. (1). This also avoids the problem of units, since K_{ad} should be dimensionless.

The $\Delta G°$ values were calculated using Eq. (9) and the values of $\Delta H°$ and $\Delta S°$ were determined from the slope and the intercept of the plots of logK_{ad} vs. 1/T shown in Fig. 17.

From the obtained thermodynamic parameters described in Table 6, all $\Delta G°$ values were negative, indicating that the adsorption of metoprolol onto BPPAC was a spontaneous process and thermodynamically favourable. Negative $\Delta H°$ value suggests the exothermic nature of adsorption while the negative value of $\Delta S°$ reveals a decreasing randomness at the solid-solution interface and the affinity of the BPPAC for metoprolol confirming a physical adsorption [70]. $\Delta G°$ values were found between 1 and 10 kJ/mol indicating that physisorption might

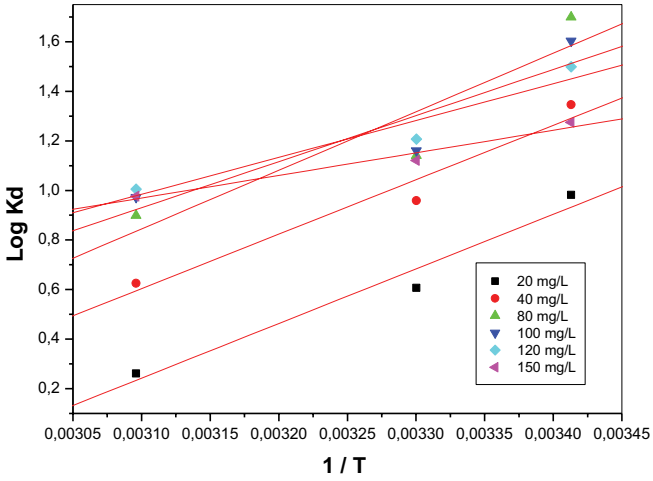

Fig. 17. Determination of thermodynamic parameters.

Table 6
Thermodynamic parameters of metoprolol adsorption

C_0	$\Delta S°$	$\Delta H°$	$\Delta G°$ (kJ/mol)		
(mg/L)	(kJ/mol)	(kJ/mol)	20°C	30°C	50°C
20	–0.126	–4.219	–5.509	–3.519	–1.615
40	–0.118	–4.206	–7.552	–5.559	–3.867
80	–0.124	–4.525	–9.531	–6.614	–5.555
100	–0.092	–3.560	–8.994	–6.734	–6.016
120	–0.069	–2.848	8.407	–7.002	–6.502
150	–0.035	–1.745	–6.016	–6.217	–6.039

Fig. 18. Desorption of metoprolol from BPPAC.

dominate the metoprolol adsorption process [71]. Similar results were reported in previous research works [72].

3.15. Desorption cycles of regeneration

Generally it is always important to examine the desorption process to recover the pollutant from the adsorbent. This did encourage the study of the regeneration of metoprolol from BPPAC, testing different eluents like HNO_3, HCl, NaOH and distilled water. Fig. 18 shows that HNO_3 was the optimum solvent and gave significant results with a desorption rate of 61.34%, from the first cycle but metoprolol adsorbed onto BPPAC might not be completely removed and during the second cycle removal efficiency decreased to 32.49%. According to the obtained results, no interesting desorption was observed in distilled water. However, in presence of NaOH and HCl, desorption percentage of metoprolol was approximately the same. However the major inconvenient of nitric acid is the fact that it is a strong oxidant and may affect the stability both of the pollutant and of the regenerated adsorbent. This point was not considered because the main objective of the present study was to remove metoprolol from wastewaters, by adsorption and the stability of the involved elements was not really of any interest.

4. Conclusion

Through this study, activated carbons were prepared from raw bean peels using phosphoric and sulphuric acids as the chemical activating agents. The obtained adsorbents were a priori assessed basing on the specific surface areas using BET technique. Values of 0.422, 38.25 and 1,100.39 m^2/g, for raw bean peels, phosphoric and sulphuric acids activated carbon, respectively, were obtained. This confirms that the activation process had improved the specific surface area of the raw bean peels by factors of 2,600 and 91 when phosphoric and sulphuric acids were used, respectively. The effects of various operating parameters like the solid–liquid ratio, the initial pH, initial concentration, the salt ionic strength, the activating agent, were investigated. The obtained results showed that the removal efficiency was greatly affected by the solution pH and the electrolyte concentration. However an optimum metoprolol removal rate of 98% was achieved at ambient temperature.

Different isotherm models were tested for the case of metoprolol adsorption onto bean peels phosphoric acid activated carbon and the corresponding determination coefficients showed that the best fit was obtained with Langmuir isotherm model, indicating monolayer coverage of metoprolol on the adsorbent surface. Adsorption of metoprolol was well described by pseudo-second-order model. The thermodynamic analysis indicated that the metoprolol adsorption onto phosphoric acid activated carbon was physical, endothermic and a spontaneous process. Desorption studies were carried out to explore the feasibility of the regeneration of the used activated carbon and it was found that up to 60% of the retained metoprolol was desorbed with 0.1 mol/L HNO_3 solution, although this latter was a strong oxidant, able to induce stability problems. Finally basing on the obtained results, the bean peels phosphoric acid activated carbon was an adequate and a performing adsorbent for the removal of metoprolol from wastewaters generated by specific sources releasing these kinds of beta-blocker compounds.

References

[1] V. Chander, B. Sharma, V. Negi, R.S. Aswal, P. Singh, R. Singh, R. Dobhal, Pharmaceutical compounds in drinking water, J. Xenobiot., 6 (2016) 5774, doi: 10.4081/xeno.2016.5774.

[2] I. Villaescusa, N. Fiol, J. Poch, A. Bianchi, C. Bazzicalupi, Mechanism of paracetamol removal by vegetable wastes: the contribution of π-π interactions, hydrogen bonding and hydrophobic effect, Desalination, 270 (2011) 135–142.

[3] J.R. Domínguez, T. González, P. Palo, E.M. Cuerda-Correa, Removal of common pharmaceuticals present in surface waters by Amberlite XAD-7 acrylic-ester-resin: influence of pH and presence of other drugs, Desalination, 269 (2011) 231–238.

[4] A. de Wilt, Y. He, N. Sutton, A. Langenhoff, H. Rijnaarts, Sorption and biodegradation of six pharmaceutically active compounds under four different redox conditions, Chemosphere, 193 (2018) 811–819.

[5] J.R. de Andrade, M.F. Oliveira, M.G.C. da Silva, M.G.A. Vieira, Adsorption of pharmaceuticals from water and wastewater using nonconventional low-cost materials: a review, J. Chem. Eng., 57 (2018) 3103–3127.

[6] R.A. Figueroa, A.A. MacKay, Sorption of oxytetracycline to iron oxides and iron oxide-rich soils, Environ. Sci. Technol., 39 (2005) 6664–6671.

[7] R.A. Figueroa, A. Leonard, A.A. MacKay, Modeling tetracycline antibiotic sorption to clays, Environ. Sci. Technol., 38 (2004) 476–483.

[8] J.R.V. Pils, D.A. Laird, Sorption of tetracycline and chlortetracycline on K- and Ca-saturated soil clays, humic substances, and clay-humic complexes, Environ. Sci. Technol., 41 (2007) 1928–1933.

[9] C. Gu, K.G. Karthikeyan, Interaction of tetracycline with aluminium and iron hydrous oxides, Environ. Sci. Technol., 39 (2005) 2660–2667.

[10] T.X. Bui, H. Choi, Influence of ionic strength, anions, cations, and natural organic matter on the adsorption of pharmaceuticals to silica, Chemosphere, 80 (2010) 681–686.

[11] J. Maszkowska, S. Stolte, J. Kumirska, P. Łukaszewicz, K. Mioduszewska, A. Puckowski, M. Caban, M. Wagil, P. Stepnowski, A. Białk-Bielińska, Beta-blockers in the environment: Part I. Mobility and hydrolysis study, Sci. Total Environ., 493 (2014) 1112–1121.

[12] R.S. Vardanyan, V.J. Hruby, Synthesis of Essential Drugs, 1st ed., Elsevier, 2006.

[13] S.N. Nanaki, G.Z. Kyzas, A. Tzereme, M. Papageorgiou, M. Kostoglou, D.N. Bikiaris, D.A. Lambropoulou, Synthesis and characterization of modified carrageenan microparticles for the removal of pharmaceuticals from aqueous solutions, Colloids Surf., B, 127 (2015) 256–265.

[14] D. Calamari, E. Zuccato, S. Castiglioni, R. Bagnati, R. Fanelli, Strategic survey of therapeutic drugs in the rivers Po and Lambro in Northern Italy, Environ. Sci. Technol., 37 (2003) 1241–1248.

[15] J. Maszkowska, S. Stolte, J. Kumirska, P. Łukaszewicz, K. Mioduszewska, A. Puckowski, M. Caban, M. Wagil, P. Stepnowski, A. Białk-Bielińska, Beta-blockers in the environment: part I. Mobility and hydrolysis study, Sci. Total Environ., 493 (2014) 1112–1121.

[16] S.J. Enna, D.B. Bylund, Eds., xPharm: The Comprehensive Pharmacology Reference, Elsevier, 2007.

[17] N. Gherbi, Z. Ziani, M. Khetib, D. Belkharchouche, A.-H. Meniai, Experimental study and test of a new biosorbent prepared from bean peels to remove Rhodamine B from industrial wastewaters, Desal. Water Treat., 221 (2021) 64–75.

[18] M. Kwiatkowski, J. Srenścek-Nazzal, B. Michalkiewicz, An analysis of the effect of the additional activation process on the formation of the porous structure and pore size distribution of the commercial activated carbon WG-12, Adsorption, 23 (2017) 551–561.

[19] M.A. Lillo-Ródenas, D. Cazorla-Amorós, A. Linares-Solano, Understanding chemical reactions between carbons and NaOH and KOH: an insight into the chemical activation mechanism, Carbon, 41 (2003) 267–275.

[20] M.P. Elizalde-González, J. Mattusch, A.A. Peláez-Cid, R. Wennrich, Characterization of adsorbent materials prepared from avocado kernel seeds: natural, activated and carbonized forms, J. Anal. Appl. Pyrolysis, 78 (2007) 185–193.

[21] A. Reffas, V. Bernardet, B. David, L. Reinert, M. Bencheikh Lehocine, M. Dubois, N. Batisse, L. Duclaux, Carbons prepared from coffee grounds by H_3PO_4 activation: characterization and adsorption of methylene blue and Nylosan Red N-2RBL, J. Hazard. Mater., 175 (2010) 779–788.

[22] C.K. Singh, J.N. Sahu, K.K. Mahalik, C.R. Mohanty, B. Raj Mohan, B.C. Meikap, Studies on the removal of Pb(II) from wastewater by activated carbon developed from *Tamarind wood* activated with sulphuric acid, J. Hazard. Mater., 153 (2008) 221–228.

[23] S. Smart, S. Liu, J.M. Serra, J.C. Diniz da Costa, A. Iulianelli, A. Basile, Chapter 8 – Porous Ceramic Membranes for Membrane Reactors, A. Basile, Ed., Handbook of Membrane Reactors: Fundamental Materials Science, Design and Optimisation, Volume 1 in Woodhead Publishing Series in Energy, Woodhead Publishing, 2013, pp. 298–336.

[24] C.F. Toncón-Leal, J. Villarroel-Rocha, M.T.P. Silva, T.P. Braga, K. Sapag, Characterization of mesoporous region by the scanning of the hysteresis loop in adsorption–desorption isotherms, Adsorption, 27 (2021) 1109–1122.

[25] J. Alcañiz-Monge, D. Lozano-Castelló, D. Cazorla-Amorós, A. Linares-Solano, Fundamentals of methane adsorption in microporous carbons, Microporous mesoporous Mater., 124 (2009) 110–116.

[26] M.S. Solum, R.J. Pugmire, M. Jagtoyen, F. Derbyshire, Evolution of carbon structure in chemically activated wood, Carbon, 33 (1995) 1247–1254.

[27] J. Gülen, F. Zorbay, Methylene blue adsorption on a low cost adsorbent-carbonized peanut shell, Water Environ. Res., 89 (2017) 805–816.

[28] L.-Y. Hsu, H. Teng, Influence of different chemical reagents on the preparation of activated carbons from bituminous coal, Fuel Process. Technol., 64 (2000) 155–166.

[29] W.-C. Tan, R. Othman, A. Matsumoto, F.-Y. Yeoh, The effect of carbonisation temperatures on nanoporous characteristics of activated carbon fibre (ACF) derived from oil palm empty fruit bunch (EFB) fibre, J. Therm. Anal. Calorim., 108 (2012) 1025–1031.

[30] V.M. Gun'ko, V.V. Turo, O.P. Kozynchenko, V.G. Nikolaev, S.R. Tennison, S.T. Meikle, E.A. Snezhkova, A.S. Sidorenko, F. Ehrburger-Dolle, I. Morfin, D.O. Klymchuk, S.V. Mikhalovsky, Activation and structural and adsorption features of

activated carbons with highly developed micro-, meso- and macroporosity, Adsorption, 17 (2011) 453–460.
[31] S.A. Mirzaee, B. Bayati, M.R. Valizadeh, H.T. Gomes, Z. Noorimotlagh, Adsorption of diclofenac on mesoporous activated carbons: physical and chemical activation, modeling with genetic programming and molecular dynamic simulation, Chem. Eng. Res. Des., 167 (2021) 116–128.
[32] N. Jaafarzadeh, Z. Baboli, Z. Noorimotlagh, S. Silva Martínez, M. Ahmadi, S. Alavi, S.A. Mirzaee, Efficient adsorption of bisphenol A from aqueous solutions using low-cost activated carbons produced from natural and synthetic carbonaceous materials, Desal. Water Treat., 154 (2019) 177–187.
[33] A. Özer, G. Dursun, Removal of methylene blue from aqueous solution by dehydrated wheat bran carbon, J. Hazard. Mater., 146 (2007) 262–269.
[34] J. Sahar, A. Naeem, M. Farooq, S. Zareen, S. Sherazi, Kinetic studies of graphene oxide towards the removal of rhodamine B and congo red, Int. J. Environ. Anal. Chem., 101 (2021) 1258–1272.
[35] R.K. Sheshdeh, M.R.K. Nikou, K. Badii, N.Y. Limaee, G. Golkarnarenji, Equilibrium and kinetics studies for the adsorption of Basic Red 46 on nickel oxide nanoparticles-modified diatomite in aqueous solutions, J. Taiwan Inst. Chem. Eng., 45 (2014) 1792–1802.
[36] M. Zamouche, L. Mouni, A. Ayachi, I. Merniz, Use of commercial activated carbon for the purification of synthetic water polluted by a pharmaceutical product, Desal. Water Treat., 172 (2019) 86–95.
[37] H. Ali, S.K. Muhammad, Biosorption of crystal violet from water on leaf biomass of *Calotropis procera*, J. Environ. Sci. Technol., 1 (2008) 143–150.
[38] N.V. Suc, D.K. Chi, Removal of rhodamine B from aqueous solution via adsorption onto microwave-activated rice husk ash, J. Dispersion Sci. Technol., 38 (2016) 216–222.
[39] O.S. Bello, K.A. Adegoke, O.O. Sarumi, O.S. Lameed, Functionalized locust bean pod (*Parkia biglobosa*) activated carbon for Rhodamine B dye removal, Heliyon, 5 (2019) e02323, doi: 10.1016/j.heliyon.2019.e02323.
[40] D. Naghipour, A. Amouei, K.T. Ghasemi, K. Taghavi, Removal of metoprolol from aqueous solutions by the activated carbon prepared from pine cones, Environ. Health Eng. Manage. J., 6 (2019) 81–88.
[41] S. Bousba, A.-H. Meniai, Adsorption of 2-chlorophenol onto sewage sludge based adsorbent: equilibrium and kinetic study, Chem. Eng. Trans., 35 (2013) 854–869.
[42] C.-H. Weng, Y.-T. Lin, T.-W. Tzeng, Removal of methylene blue from aqueous solution by adsorption onto pineapple leaf powder, J. Hazard. Mater., 170 (2009) 417–424.
[43] E.K. Guechi, Equilibrium, kinetics and mechanism for the removal of Rhodamine B by adsorption on Okoume (*Aucoumea klaineana*) sawdust from aqueous media, Desal. Water Treat., 94 (2017) 164–173.
[44] M. Daneshkhah, H. Hossaini, M. Malakootian, Removal of metoprolol from water by sepiolite-supported nanoscale zero-valent iron, J. Environ. Chem. Eng., 5 (2017) 3490–3499.
[45] M. Pedrosa, R.S. Ribeiro, S. Guerra-Rodríguez, J. Rodríguez-Chueca, E. Rodríguez, A.M.T. Silva, M. Đolic, A.R. Lado, *Spirulina*-based carbon bio-sorbent for the efficient removal of metoprolol, diclofenac and other micropollutants from wastewater, Environ. Nanotechnol. Monit. Manage., 18 (2022) 100720, doi: 10.1016/j.enmm.2022.100720.
[46] M. Ghaedi, J. Tashkhourian, A.A. Pebdani, B. Sadeghian, F.N. Ana, Equilibrium, kinetic and thermodynamic study of removal of reactive orange 12 on platinum nanoparticle loaded on activated carbon as novel adsorbent, Korean J. Chem. Eng., 28 (2011) 2255–2261.
[47] T. Shojaeimehr, F. Rahimpour, M.A. Khadivi, M. Sadeghi, A modeling study by response surface methodology (RSM) and artificial neural network (ANN) on Cu^{2+} adsorption optimization using light expended clay aggregate (LECA), J. Ind. Eng. Chem., 20 (2013) 870–880.
[48] W.J. Weber, J.C. Morris, Kinetics of adsorption on carbon from solution, J. Sanit. Eng. Div. ASCE, 89 (1963) 31–59.
[49] S.S. Vieira, Z.M. Magriotis, N.A.V. Santos, M. das Graças Cardoso, A. Saczk, Macauba palm (*Acrocomia aculeata*) cake from biodiesel processing: an efficient and low cost substrate for the adsorption of dyes, Chem. Eng. J., 183 (2012) 152–161.
[50] S. Zafara, Kinetic, equilibrium and thermodynamic studies for adsorption of nickel ions, Desal. Water Treat., 167 (2019) 277–290.
[51] S.H. Chien, W.R. Clayton, Application of Elovich equation to the kinetics of phosphates release and sorption in soils, Soil Sci. Soc. Am. J., 44 (1980) 265–268.
[52] F. Deniz, D.S. Saygideger, Investigation of adsorption characteristics of Basic Red 46 onto gypsum: equilibrium, kinetic and thermodynamic studies, Desalination, 262 (2010) 161–165.
[53] A. Benhouria, M.A. Islama, H. Zaghouane-Boudiaf, M. Boutahala, B.H. Hameed, Calcium alginate–bentonite–activated carbon composite beads as highly effective adsorbent for methylene blue, Chem. Eng. J., 270 (2015) 621–630.
[54] L. Largitte, R. Pasquier, A review of the kinetics adsorption models and their application to the adsorption of lead by an activated carbon, Chem. Eng. Res. Des., 109 (2016) 495–504.
[55] C.H. Giles, D. Smith, A. Huiston, A general treatment and classification of the solute adsorption isotherm, J. Colloid Interface Sci., 47 (1974) 755–765.
[56] C.H. Giles, T.H. MacEwan, S.N. Nakhwa, D. Smith, 786. Studies in adsorption. Part XI. A system of classification of solution adsorption isotherms, and its use in diagnosis of adsorption mechanisms and in measurement of specific surface areas of solids, J. Chem. Soc. (Resumed), 11 (1960) 3973–3993.
[57] S.N. Souissi, A. Ouderni, A. Ryel, Adsorption of dyes onto activated carbon prepared from olive stone, J. Environ. Sci., 17 (2005) 998–1003.
[58] P. Senthil Kumar, S. Ramalingam, C. Senthamarai, M. Niranjanaa, P. Vijayalakshmi, Adsorption of dye from aqueous solution by cashew nut shell: studies on equilibrium isotherm, kinetics and thermodynamics of interactions, Desalination, 261 (2010) 52–60.
[59] B. Belhamdi, Z. Merzougui, M. Trari, A. Addoun, A kinetic, equilibrium and thermodynamic study of L-phenylalanine adsorption using activated carbon based on agricultural waste (date stones), J. Appl. Res. Technol., 14 (2016) 354–366.
[60] Z. Anfar, M. Zbair, H. Ait Ahsaine, M. Ezahri, N. El Alem, Well-designed WO_3/activated carbon composite for Rhodamine B removal: synthesis, characterization, and modelling using response surface methodology, Fullerenes Nanotubes Carbon Nanostruct., 26 (2018) 389–397.
[61] V. Vimonses, S.M. Lei, B. Jin, C.W.K. Chow, C. Saint, Kinetic study and equilibrium isotherm analysis of Congo Red adsorption by clay materials, Chem. Eng. J., 148 (2009) 354–364.
[62] H. Freundlich, Over the adsorption in solution, J. Phys. Chem., 57 (1906) 358–471.
[63] J. Guo, S. Chen, L. Liu, B. Li, P. Yang, L. Zhang, Y. Feng, Adsorption of dye from wastewater using chitosan–CTAB modified bentonites, J. Colloid Interface Sci., 382 (2012) 61–66.
[64] J.F. Duarte Neto, I.D.S. Pereira, V.C. da Silva, H.C. Ferreira, G. de A. Neves, R.R. Menezes, Study of equilibrium and kinetic adsorption of Rhodamine B onto purified bentonite clays, Cerâmica, 64 (2018) 598–607.
[65] L.Z. Lee, M.A.A. Zaini, Rhodamine B dyes adsorption on palm kernel shell based activated carbons, Malaysian J. Fundam. Appl. Sci., 15 (2019) 743–747.
[66] M.C. Ncibi, A.M. Ben Hamissa, A. Fathallah, M.H. Kortas, T. Baklouti, B. Mahjoub, M. Seffen, Biosorptive uptake of methylene blue using Mediterranean green alga *Enteromorpha* spp., J. Hazard. Mater., 170 (2009) 1050–1055.
[67] J. Shah, M. Rasul Jan, A. Haq, Y. Khan, Removal of Rhodamine B from aqueous solutions and wastewater by walnut shells: kinetics, equilibrium and thermodynamics studies, Front. Chem. Sci. Eng., 7 (2013) 428–436.
[68] K. Fujiwara, A. Ramesh, T. Maki, H. Hasegawa, K. Ueda, Adsorption of platinum (IV), palladium (II) and gold (III) from aqueous solutions onto L-lysine modified crosslinked chitosan resin, J. Hazard. Mater., 146 (2006) 39–50.
[69] S. Doyurum, A. Celik, Pb(II) and Cd(II) removal from aqueous solutions by olive cake, J. Hazard. Mater., 138 (2006) 22–28.

[70] B.H. Hameed, Equilibrium and kinetics studies of 2,4,6-trichlorophenol adsorption onto activated clay, Colloids Surf., A, 307 (2007) 45–52.
[71] T. Phatthanakittiphong, G.T. Seo, Characteristic evaluation of graphene oxide for Bisphenol A adsorption in aqueous solution, Nanomaterials (Basel), 6 (2016) 128, doi: 10.3390/nano6070128.
[72] K. Vijayaraghavan, Y.-S. Yun, Biosorption of C.I. Reactive Black 5 from aqueous solution using acid-treated biomass of brown seaweed *Laminaria* sp., Dyes Pigm., 76 (2008) 726–732.